SMiRT-12 / K. Kussmaul (Editor)

L05/1

CREEP-FATIGUE DAMAGE ASSESSMENT BY SUBSEQUENT FATIGUE STRAINING

M. Yaguchi, T. Nakamura, A. Ishikawa and Y. Asada

Department of Mechanical Engineering, The University of Tokyo, 7-3-1 Hongo, Bunkyo-ku, Tokyo 113, Japan

ABSTRACT

A series of creep-fatigue tests has been conducted with Modified 9Cr-1Mo steel at 600 °C in a high vacuum environment of 0.1mPa to assess an accumulation of creep-fatigue damage. In these tests, each test specimen has been subjected to prior creep-fatigue loading followed by subsequent fatigue loading or prior fatigue loading followed by subsequent creep-fatigue loading. A linear summation of cumulative damage of fatigue and creep life fraction is smaller than unity for the former case, and larger than unity for the latter case. SEM observation was conducted and it was shown that in the case of prior creep-fatigue loading, crack mode transforms from transgranular to intergranular type with the increase of the number of cycles of prior creep-fatigue loading, while crack mode is generally intergranular in the case of prior fatigue loading.

1. INTRODUCTION

A precise evaluation of creep-fatigue damage is an important problem in the high temperature structural design. In previous studies and the authors' (Morishita and Asada, 1984; Morishita et al., 1987; Asayama and Asada, 1989; Okamoto et al., 1991) ones on this problem, it is usually assumed that the creep damage and the fatigue damage are linearly summed to express the creep-fatigue interaction and that the damage accumulates linearly with respect to loading cycles. But it is not clear if these simple assumptions are valid to make a precise and realistic description of the creep-fatigue interaction. The present study is focused on the latter assumption.

A series of creep-fatigue tests has been conducted with Modified 9Cr-1Mo steel at 600 °C in a high vacuum environment of 0.1 mPa to assess an accumulation of creep-fatigue damage. The high vacuum environment was employed to avoid the environmental effect of air on the creep-fatigue damage(Asada et al., 1992). Contrary to the usual creep-fatigue tests where strain-time program is held constant until failure, the creep-fatigue tests in this study were conducted with prior creep-fatigue loading followed by subsequent fatigue loading and with prior fatigue loading followed by subsequent creep-fatigue loading at the same strain range to study the accumulation of creep-fatigue damage. SEM observation was also conducted to discuss the test results from the view point of fractography.

2. EXPERIMENTS

2.1 Material

The test material is a normalized and tempered Modified 9Cr-1Mo steel. Chemical composition and the condition of heat treatment are shown in Table 1.

2.2 Test facility

The test facility is a hydraulic closed loop system with an induction heating device and a vacuum system. The vacuum system consists of a diffusion pump and a rotatory pump and can attain a high vacuum of 0.1 mPa. Stress-strain-time data were sampled and stored with a PC for further analyses.

2.3 Test condition

A series of tests was made under a controlled push-pull strain at 600°C in a high vacuum environment of 0.1 mPa. As shown in Fig.1, two kinds of loading types were employed; (A) prior creep-fatigue loading with subsequent fatigue loading, (B) prior fatigue loading with subsequent creep-fatigue loading.

In the type (A) loading, three types of creep-fatigue strain wave forms were used to examine the effect of the wave form on the accumulation of creep-fatigue damage. The wave forms for the creep-fatigue loading are as follows; a slow tension-fast compression with tensile strain rate/compressive strain rate = $10^{-4}/10^{-3}$ s^{-1} and $10^{-5}/10^{-3}$ s^{-1} and a tensile strain hold cycle with a strain rate of $10^{-3}/10^{-3}s^{-1}$ and a strain hold time t_h of 600 s. The wave form of the fatigue loading is a symmetric continuous cycle with a strain rate of $10^{-3}/10^{-3}$ s^{-1}. A strain range was held constant through the test at either 0.01 or 0.02.

In the type (B) loading, the prior fatigue cycle has a strain rate of $10^{-3}/10^{-3}s^{-1}$. The subsequent creep-fatigue loading is a slow tension-fast compression type with a strain rate of $10^{-4}/10^{-3}$ s^{-1}. A strain range was held constant through the test at 0.01.

3. RESULTS

In this study, n_1 and n_2 mean the number of cycles of prior loading and that of subsequent loading, respectively. N_1 and N_2 mean the number of cycles to failure of prior loading condition and that of subsequent loading condition. Therefore, "n_1/N_1" stands for a life fraction of prior loading and "n_2/N_2" stands for that of subsequent loading.

3.1 Stress-strain response

Figure 2-1 shows the example of cyclic response of a peak stress in the case of type (A) loading (prior creep-fatigue loading followed by fatigue loading). It is interesting that the maximum stress of type (A) loading took the same value as that of pure fatigue loading at the same number of cycle after the strain wave form changed from the prior creep-fatigue loading to the subsequent fatigue loading.

Figure 2-2 shows the example of cyclic response of peak stress in the case of type (B) loading (prior fatigue loading followed by creep-fatigue

loading). The maximum stress approximately took the same value as that of pure creep-fatigue loading at the same number of cycle after the wave form changed from the prior fatigue loading to the subsequent creep-fatigue loading.

3.2 Analysis of cumulative damage

Figure 3 shows the test results in terms of "n_1/N_1" vs. "n_2/N_2" relation. The solid line in Fig.3 means that the linear cumulative damage D which is defined by eq.(1) is equal to unity.

$$D = \frac{n_1}{N_1} + \frac{n_2}{N_2} \qquad (1)$$

3.2.1 Type (A) loading

In the case of type (A) loading, the cumulative damage D is smaller than unity in all cases as shown in Fig.3. The value of D takes minimum when "n_1/N_1" equals to 0.2. A bilinear line was fitted to the test data as shown by broken line in Fig.3.

The subsequent fatigue life fraction is lower when an applied strain range is smaller, however there observed no definite trend in life reduction due to the strain wave form. When the strain range equals to 0.01, type (A-2) loading gives the biggest difference from the linear rule, but when the strain range equals to 0.02, type (A-1) loading gives the biggest difference.

3.2.2 Type (B) loading

In the case of type (B) loading, the cumulative damage D is larger than unity when "n_1/N_1" is equal to 0.25 and 0.50, however, smaller than unity when "n_1/N_1" is equal to 0.75, as shown in Fig.3.

4. SEM OBSERVATION

4.1 Type (A) loading

Differing from the case of pure fatigue loading, the main crack propagated not from the surface of the specimen but from the inside of the specimen.

SEM observation was made on the site from which the crack propagated. In the case of "n_1/N_1" is smaller than 0.5 the crack propagated from an inclusion around which there were cavities as shown in Fig.4-1, and the crack propagated from a site of a wrinkled feature as well as from the inclusion in the case of "n_1/N_1" is larger than 0.5, as shown in Fig.4-2.

With an increase of "n_1/N_1", the feature of crack propagation was observed to transform from transgranular type to intergranular type.

4.2 Type (B) loading

In the cases that "n_1/N_1" is equal to 0.25 and 0.50, the fracture surface predominantly showed the intergranular crack mode and the crack propagated from the inclusion or the site of the wrinkled feature. Whereas "n_1/N_1" equals to 0.75, the crack propagated from the surface of the specimen and the crack mode was transgranular.

5. DISCUSSION

5.1 Type (A) loading

In this case, the test result showed that the linear cumulative damage D is smaller than unity.

The SEM observation showed that the crack propagated form the inclusion around which there were many cavities or from the site of the wrinkled feature and the crack mode transformed from transgranular to intergranular type with an increase of "n_1/N_1". In the previous study(Okamoto et al., 1991) on the creep-fatigue behavior of this material, it was found out that in the high vacuum environment there exist following two features.

(a) In the case of pure fatigue loading, the crack which initiates on the surface of the specimen propagates with the transgranular mode and no creep cavity is observed.

(b) In the case of creep-fatigue loading, the crack which initiates inside the specimen generally shows intergranular mode and cavities are observed on the intergranular crack.

Therefore, it can be said that the cavities observed around the crack initiation site were generated during prior creep-fatigue loading and played the roll of the initial micro-crack for the subsequent fatigue loading. That is, in the subsequent fatigue loading, it is suggested that the micro-cracks had already been created by the prior creep-fatigue loading. The subsequent fatigue cycles were spent almost for the crack propagation.

In the case of type (A) loading, the "n_2/N_2" in eq.(1) means the cumulative fatigue damage at the number of cycle of n_2. Attention should be paid to the fact that N_2 contains both the crack initiation period and propagation period. It is suggested that in "n_2/N_2" of eq.(1) a propagation stage is underestimated since N_2 is larger than the crack propagation life which should be used to evaluate the subsequent fatigue damage, and that it results in the cumulative damage smaller than unity.

5.2 Type (B) loading

The test result showed that the linear cumulative damage D is generally larger than unity.

The SEM observation showed that the crack mode is predominantly intergranular. The subsequent creep-fatigue loading generated this intergranular fracture mode because no intergranular fracture was observed for the pure fatigue case in the authors' previous study (Okamoto et al., 1991).

By the fact that the predominant fracture mode is intergranular and that the linear cumulative damage rule gives the damage larger than unity, it is suggested that the transgranular crack which initiated during the prior loading has less effect on the initiation and propagation of the fatal intergranular crack during the subsequent creep-fatigue loading.

6. CONCLUSIONS

A series of creep-fatigue test was conducted with Modified 9Cr-1Mo steel at 600 °C in a high vacuum environment in order to assess an accumulation of creep-fatigue damage. In these tests, each test specimen has been subjected to prior creep-fatigue loading followed by subsequent fatigue loading or prior fatigue loading followed by subsequent creep-fatigue

loading. Following conclusions were obtained.

A linear cumulative damage rule gives the summation fo the life fraction smaller than unity in the case of prior creep-fatigue loading followed by subsequent fatigue loading, and larger than unity in the case of prior fatigue loading followed by subsequent creep-fatigue loading.

In the case of prior creep-fatigue loading followed by the fatigue loading, the crack mode transformed from transgranular to intergranular type with an increase of prior creep-fatigue loading cycles. In the case of prior fatigue loading followed by the subsequent creep-fatigue loading, a fracture surface predominantly showed intergranular crack.

It is suggested that the life fraction summation becomes smaller than unity when the crack initiation duration reduce itself due to the cavity creation by the prior creep-fatigue loading and that life fraction summation becomes larger than unity when the fatigue crack initiated during the prior fatigue loading does not have so much effect on the subsequent damage of the intergranular mode.

REFERENCES

Morishita, M. and Asada, Y., (1984) NED Vol.83 pp.367-377.
Morishita, M., Taguchi, K., Asayama, T., Ishikawa, A. and Asada, Y., (1987) ASTM STP 942 pp.487-499.
Asayama, T. and Asada, Y.,(1989) Trans. SMiRT 10, Vol.L pp.109-114.
Okamoto, Y., Yaguchi, M., Ishikawa, A., Asada, Y. and Asayama, T.,(1991) Trans. SMiRT 11, Vol.L pp.349-354.
Asada, Y., Nakamura, T., Yaguchi, M., Ishikawa, A. and Cao, G.,(1992) ASME PVP-Vol.230, pp.47-52.

Table 1 Chemical Composition of Modified 9Cr-1Mo steel (wt%)

C	Si	Mn	P	S	Ni	Cr	Mo	Nb	V	V,Al	N
0.08	0.26	0.45	0.006	0.001	0.10	8.89	0.95	0.08	0.22	0.006	0.0663

*1 50 mm Thickness Plate
*2 Normalizing: 1060°C x 60 min, Tempering: 760°C x 60 min

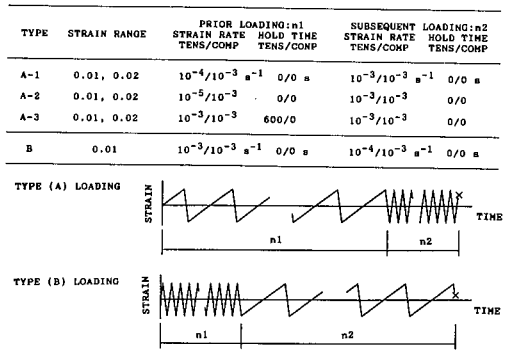

Fig.1 Strain Wave Forms for Creep-Fatigue Test

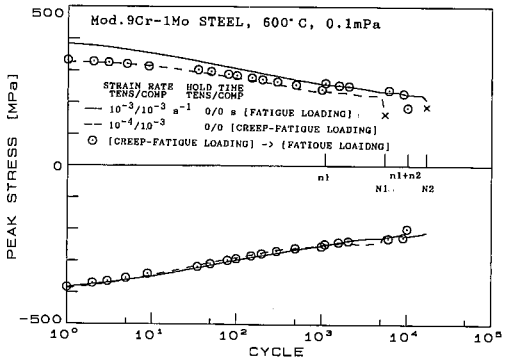

Fig.2-1 Type A-1, $n_1/N_1=0.20$, $\varepsilon_{tr}=0.01$

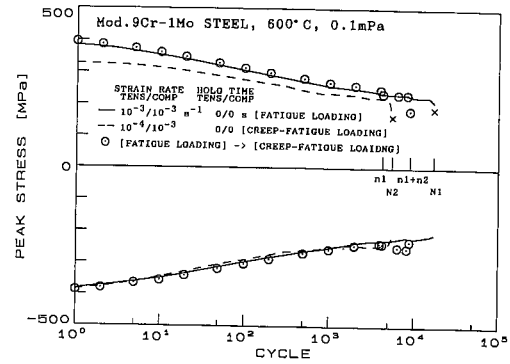

Fig.2-2 Type B, $n_1/N_1=0.25$, $\varepsilon_{tr}=0.01$

Fig.2 Cyclic Response of Peak Stress

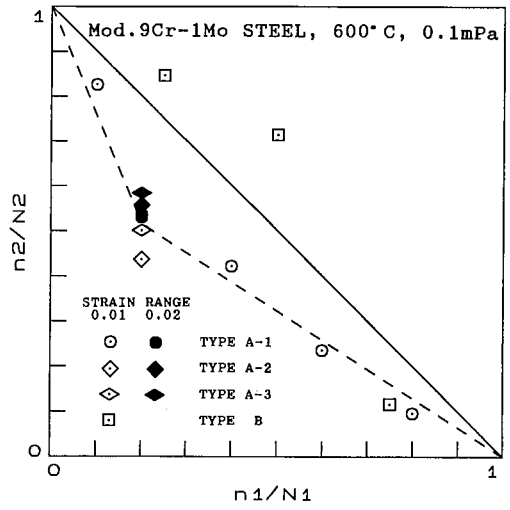

Fig.3 Results of Creep-Fatigue Test

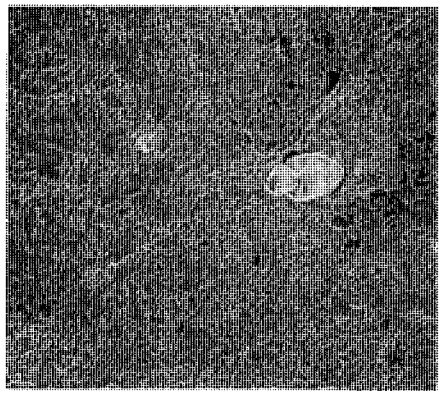

Fig.4-1 Inclusion and Cavities (Type A-1, $n_1/N_1=0.40$, $\varepsilon_{tr}=0.01$)

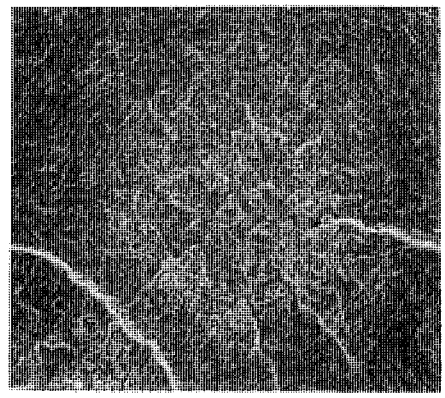

FIg.4-2 Site of Wrinkled Feature (Type A-1, $n_1/N_1=0.80$, $\varepsilon_{tr}=0.01$)

Fig.4 SEM Observation